

## Pinning of Adsorbed Cobalt Atoms by Defects Embedded in the Copper (111) Surface

Erik Zupanič,<sup>1</sup> Rok Žitko,<sup>1,2</sup> Herman J. P. van Midden,<sup>1</sup> Igor Muševič,<sup>1,2</sup> and Albert Prodan<sup>1</sup>

<sup>1</sup>*J. Stefan Institute, Jamova 39, SI-1000 Ljubljana, Slovenia*

<sup>2</sup>*Faculty of Mathematics and Physics, University of Ljubljana, Jadranska 19, SI-1000 Ljubljana, Slovenia*

(Received 4 March 2010; published 14 May 2010)

Using a low-temperature scanning tunneling microscope (STM), we observe that Co adatoms are unusually strongly bound to a particular type of pinning centers on the Cu(111) surface. Using density-functional-theory calculations, the pinning centers are identified as Ag substitutional atoms embedded in the topmost atomic layer of the surface. These impurities are hardly detectable in the STM images as they have low topographic height and produce no standing-wave patterns. They do not affect the exchange coupling of the Co adsorbate with the substrate electrons; thus, the Kondo resonances measured on pinned and free Co adatoms show no detectable differences. Whereas free Co adatoms undergo significant surface diffusion already above 8 K, Ag-stabilized Co adatoms remain pinned up to 12.7 K.

DOI: [10.1103/PhysRevLett.104.196102](https://doi.org/10.1103/PhysRevLett.104.196102)

PACS numbers: 68.55.Ln, 61.72.Yx, 68.37.Ef, 68.43.Jk

Semiconductor and metal surfaces are intensely studied as substrates in single-atom and single-molecule manipulation and restructuring experiments [1]. Low-temperature scanning tunneling microscope (STM) can be used to assemble artificial nanostructures and measure their properties [2,3]: it reveals the surface topography with atomic resolution and probes the local density of states (LDOS) of clean and adsorbate-covered surfaces with unprecedented spatial and energy resolution [4]. Single-atom manipulation has been used, for example, to construct quantum corrals [5,6], induce chemical reactions [7], study adatom chains [8,9], and explore the exchange interaction between magnetic impurities and metallic host structure [10–12]. In spite of the enormous progress in this field, thermal stabilization of artificially assembled nanostructures remains a salient open problem.

In this Letter we report that naturally occurring defects embedded in the Cu(111) surface act as pinning centers for deposited Co atoms. Whereas Co atoms on clean Cu(111) surface show strongly enhanced surface diffusion above 8 K, their thermal motion becomes suppressed up to 12.7 K if they are pinned to an embedded defect. Using density-functional-theory (DFT) calculations, these defects were identified as Ag substitutional atoms in the topmost atomic layer. This proposition was further experimentally corroborated by controlled deposition of Ag dopants and annealing. The Ag defects are virtually unobservable with STM topography and scanning tunneling spectroscopy (STS) because of their low apparent height and the complete absence of standing-wave patterns of surface-state electrons. Furthermore, the Ag defects have no effect on the Kondo resonance spectra of pinned Co adatoms. The structure of pinned Co pairs and the temperature-dependent diffusion of Co adsorbates have been also studied: their depinning and surface mobility were followed by successive STM imaging. The results indicate that the Ag defects increase the thermal stability of the adsorbates without affecting their electronic and magnetic properties.

A high-purity Cu(111) single-crystal substrate [13] was cleaned in ultrahigh vacuum ( $<10^{-11}$  hPa) by a very thorough procedure of Ar<sup>+</sup> ion sputtering and annealing cycles. The sample was then transferred into the STM chamber and cooled to the working temperature of 7 K. Submonolayer amounts of Co atoms were deposited onto the surface from a thoroughly degassed Co wire (99.995%), wound around a Mo filament (99.95%). During the short evaporation period of about 10 s, the temperature of the sample temporarily rose from 7 to 11 K. The  $dI/dV(V)$  signal was obtained by means of the lock-in technique with a voltage modulation of 1–10 mV<sub>rms</sub> at 670 Hz. The electrochemically etched W tip was reconditioned by controlled tip-sample interaction until the images of adatoms were spherical and the STS spectra on the bare surface showed generic Cu(111) features with no spurious sharp features near zero bias.

Topographic constant-current STM images of a clean ordered Cu(111) surface show large flat terraces with a small amount of impurities which are either adsorbed on the surface or embedded in the topmost and subsurface crystal layers. After deposition, isolated Co atoms appear in the images as  $\sim 80$  pm high bumps and they show characteristic standing waves in the form of concentric rings [14]. When recorded at low enough temperature, the adatoms remained at fixed positions. At higher temperatures most of them start to diffuse while others, surprisingly, stay stable. The reason for their stability was studied in more detail by performing controlled atomic manipulations. After the tip was lowered towards the pinned Co atom, the atom was pulled away from its site by laterally repositioning the STM tip, as shown by the arrow in Fig. 1(a). With the adatom removed, the STM images revealed a faint feature at the position where the Co atom had been previously located, as indicated in Fig. 1(b). The apparent height of this feature is merely  $\sim 8$  pm. In addition, no standing-wave pattern is visible around it. The defects must be embedded in the surface, as an adsorbate

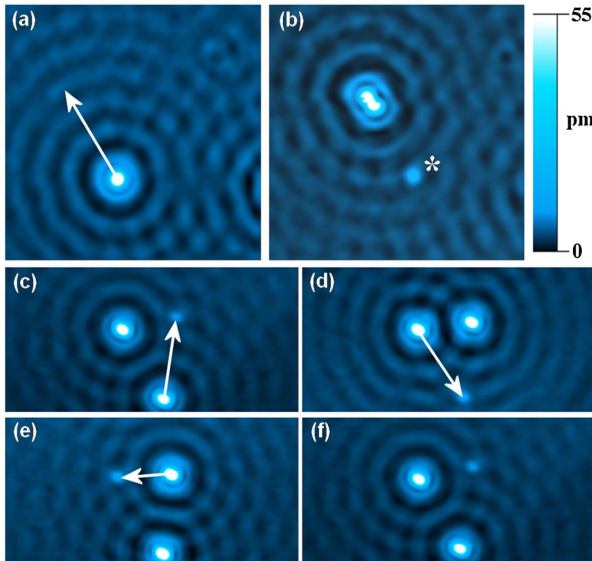


FIG. 1 (color online). (a),(b) Lateral manipulation of a Co adatom reveals an embedded defect (marked by \*) at the pinning center. Above 8 K, the position of a depinned Co adatom is unstable and the atom appears blurred. The distance between the two discernible adsorbate positions in (b) is  $0.26 \pm 0.04$  nm, which corresponds to the distance between two fcc binding sites. (c)–(f) The adatoms can be reversibly manipulated between three embedded defects. ( $I = 0.55$  nA,  $U = 30$  mV,  $T = 9$  K).

on the surface typically exhibits not only large apparent height, but also produces significant standing-wave patterns. The conjecture of embedded substitutional impurity atoms is further supported by the fact that the defect cannot be moved by the STM manipulation techniques. By carefully varying different parameters of the sample preparation procedure, it was asserted that these impurities occur naturally and do not arise as sample contamination during preparation or sample transfer.

The Co adatoms can be displaced reversibly between different defect sites with the STM tip, as demonstrated in Figs. 1(c)–1(f). The tunneling gap resistance needed to pull a Co adatom onto the defect site (or remove it from that position) is slightly lower than the one needed to manipulate it on a defect-free surface: the adatom has to overcome an additional potential barrier before it is pinned above an impurity. The Co adatoms, which had been displaced from the pinning sites are positionally unstable, show apparent height reduced by around 4 pm, undergo random jumps between neighboring adsorption sites, and appear blurred as visible in Fig. 1(b). When the rest time of the Co adatom at a certain surface site is much longer than the image acquisition time (i.e., 20 s), the Co adatom appears as a sharp circular bump, surrounded by discernible concentric standing waves, Fig. 1(a). If, however, the rest time is comparable to the image recording time, the adatom appears as a combination of images with the adatom located at different surface sites, Fig. 1(b). The probability for such displacements increases with higher bias voltages.

Figure 2(a) presents a Cu(111) surface with different types of defects usually observed on this surface. The Co pinning sites are the two faint white defects which are in sharp contrast to the other defects. Their apparent height is only  $\sim 8$  pm at 0.1 V bias voltage [Fig. 2(b)] and there is no standing-wave pattern around them [Fig. 2(a)]. Only at very high bias does the effective height increase (see Fig. 1 in the supplementary information [15]), but still without concentric rings.

The differences between the STS spectra recorded above a clean defect-free surface area and above the defects under study was found to be insignificant around Fermi level and is increasing with higher positive bias voltages (see Fig. 2 in the supplementary information [15]). The embedded impurities were also studied with spatially resolved STS mapping at different energies, which is a powerful and very discerning approach for studying electron scattering [16]. Again, no standing waves were detected in the entire voltage range of stable STM operation. These results strongly indicate that the scattering phase shift is very small in a rather wide energy interval around the Fermi level, which is highly unusual. This is a clear indication of the chemical similarity between the host Cu atoms and the impurity atom.

We have also studied the effect of embedded defects on the magnetic coupling. We found that the defects have no influence on the Kondo effect observed on a pinned Co adatom. The Kondo effect is characterized by a sharp zero-bias feature in the spectroscopy curves [6,10,11,17]. The STS spectra were carefully measured around  $E_F$  in order to determine any eventual effect of the embedded defects on the exchange coupling between the localized spin and the conduction-band electrons. The differences are, however,

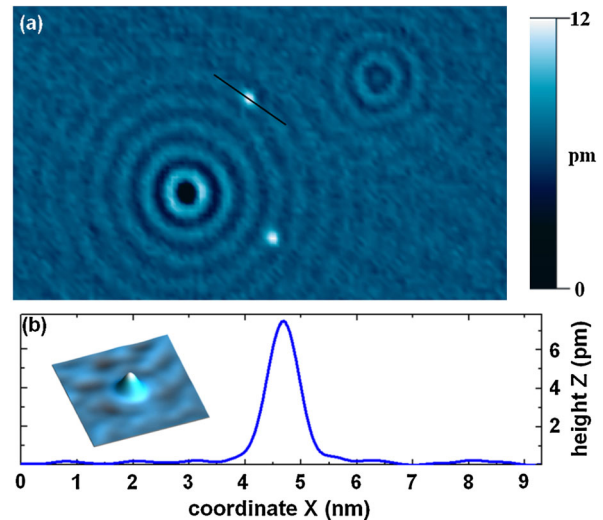


FIG. 2 (color online). (a) Topographic LT-STM image ( $35 \times 26$  nm<sup>2</sup>) of typical defects on Cu(111) surface ( $T = 7$  K,  $I = 1$  nA,  $U = 100$  mV). The embedded defects (white spots) show no standing-wave patterns. (b) Line profile across the embedded defect recorded at gap voltage of +100 mV (1 nA tunneling current) showing an apparent height of only  $\sim 8$  pm.

imperceptible: the Fano-resonance line-shape features in the tunneling spectra recorded with the STM tip over trapped cobalt adatom show no significant differences compared to those of a free cobalt adatom (see supplementary information [15], Fig. 3). This is surprising with regard to the high (exponential) sensitivity of the Kondo temperature on the atomic parameters.

By laterally manipulating an adatom onto the defect position from different directions, all possible sites of the Co adatom relative to the defect were determined as shown in Fig. 3(a). The measured distance between the defect and the Co pinning sites of  $0.26 \pm 0.04$  nm corresponds to the distance between the substitutional defect and three fcc and three hcp interstitial sites on the Cu(111) surface (Fig. 3). These sites are not the nearest-neighbor interstitial sites, but rather the next-nearest-neighbor sites.

The surface diffusion of a Co adatom which is not pinned to any defect (“free” adatom) was monitored in more detail at different temperatures by tracking its position during a slow (10 mK per minute) temperature sweep from 8.2 to 9.5 K. The scanning was always performed with low bias voltages ( $U < 10$  mV) to avoid STM tip induced motion of the adsorbates. Consecutive images were recorded at two-minute intervals and immobile surface defects provided markers for tracking the position of the mobile adatom. Its trajectory and the corresponding displacement lengths between consecutive scans are shown in Fig. 4. At temperatures from 8.2 to  $\sim 8.8$  K, the adatom jumps between adjacent binding sites, which correspond to the jump distance of  $0.26 \pm 0.04$  nm [18]. At elevated temperatures, the enlarged diffusion rate results in longer displacements between consecutive images. In a similar temperature sweep for a pinned Co adatom, the adatom position is fixed up to 12.7 K, see red squares in Fig. 4.

For a pinned Co adatom there is no telegraph noise in the tunneling spectra when the tip is positioned above the adatom and the feedback is turned off, even at high bias voltages ( $U < 100$  mV). We observed such noise for free adatoms already at 7 K for bias voltages over 5 mV and it

corresponds to random hopping between the preferred fcc binding site and the nearest-neighbor hcp sites due to inelastic electron tunneling [18]. For pinned adatoms such processes are suppressed due to the additional binding by the embedded impurity.

To compare the effect of different substitutional defects in the topmost layer of the Cu(111) surface on the electron structure in its vicinity, we have performed extensive computational studies using the DFT [19,20]. We used PWSCF code with a plane-wave basis set, ultrasoft pseudopotentials, and GGA exchange-correlation functional [21–23]. The LDOS at the Fermi level was calculated in a plane 0.21 nm above the topmost layer of surface Cu atoms. This distance roughly corresponds to the distance between the STM tip and the sample surface during scanning. The substrate surface was modeled using a three-layer slab geometry with the fcc (111) layer stacking perpendicular to the  $z$  axis, the width of the vacuum region was 1.25 nm. A 4-by-4 supercell was used along the  $x$  and  $y$  directions; such a relatively large size of the supercell is required to correctly evaluate the lateral extent of the surface area where the LDOS is perceptibly perturbed by the defect. The lattice constant was optimized so that the energy of a clean Cu slab with fully relaxed interlayer distances was minimized, yielding  $a = 0.362$  nm. In subsequent calculations, the Cu atoms in the bottom-most layer were fixed, while all other atoms were still allowed to relax; at convergence, the smallest force was below 50 meV/nm. The geometry relaxation was found to be essential to obtain reliable adsorbate binding energies. The calculations were performed for a large number of conceivable substitutional defects, including the known possible contaminants in the bulk crystal (Ag, Fe, Zn, Cr, Ca), the common surface contaminants on copper (C, O, S), as well as other transition metal atoms in the neighborhood of copper in the periodic system (Ni, Pd, Pt, Au) and some other elements. Among the likely impurities, only Ag and Zn substitutional atoms were found to induce a small change in LDOS which decays very rapidly away from the defect site (see Figs. 4 and 5 in supplementary information [15]). Other atoms yielded either a large change of the LDOS at the defect site (in some cases even of the opposite sign) or a perturbation with long-ranging tails, suggestive of a standing-wave pattern; neither of these cases agrees with the experimental results.

Using the DFT, we have also studied the adsorption energetics. The calculated binding energy for a Co adatom on the clean surface is 3.222 eV for a fcc binding site, and 8 meV less for a hcp binding site, in agreement with previous studies [18]. The binding energy for a pinned Co adatom on a fcc binding site adjacent to an Ag defect is 3.315 eV, and 3.308 eV on a hcp binding site. Thus, the cobalt adatom effectively binds to the Ag defect with an additional energy of around 90 meV. The binding energy for a Co adatom adjacent to a Zn defect is, however, only 2.3 eV, which means that the Co adatom is actually repelled from the hypothetical Zn defect. From these results, as well

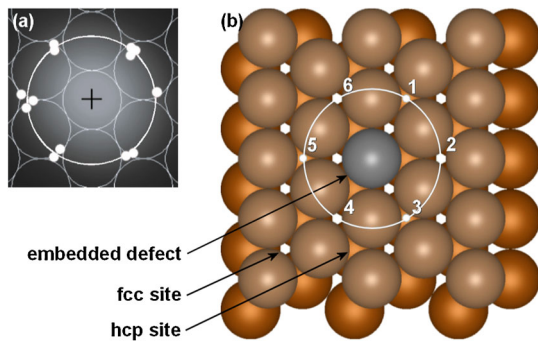


FIG. 3 (color online). (a) White dots are the experimentally determined binding sites of Co adatoms relative to the defect position. (b) Top view of the model Cu(111) surface with an embedded defect. The adatom always occupies one of the six numbered fcc and hcp sites on the surface.

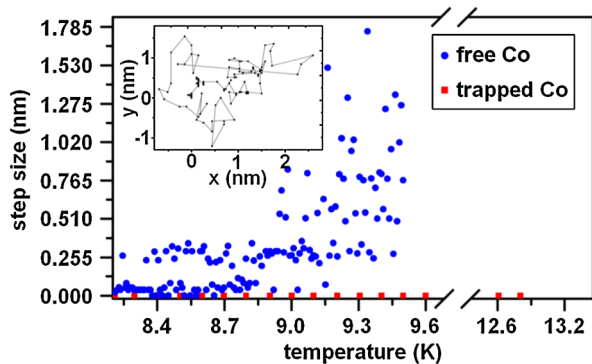


FIG. 4 (color online). Surface diffusion of a “free” Co adatom on Cu(111) (blue filled circles) and the stability of a pinned Co adatom (red squares) at different temperatures. The step size is the distance between the positions of the particle in two consecutive images. The time interval between two images (data points) is 120 sec. Note the discrete values of the displacements. The inset shows the recorded trajectory of the Co adatom during surface diffusion. The random motion of the Co adatom is not influenced by the STM tip, as the scanning direction is always from left to right and from top to bottom, whereas the displacements show no systematic drift.  $U = 10$  mV,  $I = 0.88$  nA.

as from general theoretical considerations on the similarity of chemical properties of elements differing only in having additional completely filled shells, it was concluded that the distinctive impurities can only be Ag atoms.

To confirm this theoretical prediction we have performed controlled deposition of Ag on a clean Cu (111) surface, followed by an annealing step performed with similar parameters as during the standard Cu surface cleaning procedure. Topographic images of such surface showed a strongly increased concentration of pinning centers (see Fig. 6 in the supplementary information [15]) which had the same topographic and spectroscopic characteristics as the native pinning centers.

If the concentration of deposited Co atoms exceeds that of the embedded defects, STM images reveal the formation of cobalt pairs with adatoms separated by  $0.56 \pm 0.04$  nm (see supplementary information [15], Fig. 7). This distance corresponds to that between the opposite fcc and hcp sites next to the Ag defect. The pairs are stable and always oriented along one of the three equivalent  $\langle 10\bar{1} \rangle$  directions. By removing the two adatoms, the embedded defect is revealed exactly halfway between them. Stable pairs at temperatures above 8 K can be constructed from free Co adatoms by manipulating them to the corresponding binding sites. DFT calculations show that there is some energy gain associated with the pair formation, although it is small: 13 meV.

In conclusion, we have used a low-temperature STM to study the surface stability of Co adatoms on Cu(111) surface. We have found that some of the adatoms are surprisingly stable: whereas most of the Co adatoms start diffusing already above 8 K, a small number of Co adatoms remain pinned up to 12.7 K. It was found that these adatoms

are positionally stabilized by impurity atoms which are embedded in the underlying Cu(111) surface. These atoms show no standing-wave patterns, they are hardly observable in the topographic images and do not affect the exchange coupling of the magnetic adsorbates with the substrate electrons. Using DFT calculations, they were identified as embedded Ag impurities. This prediction was further confirmed by deposition experiment. Our observation of enhanced stability of Co adatoms on Ag impurities suggests the exciting possibility of using embedded defects as templates for building artificial atomic structures, which would remain stable at elevated temperatures. Furthermore, our results indicate that ordered surface alloys might support the self-assembly of magnetic impurity lattices.

The authors acknowledge the support of the Slovenian Research Agency (ARRS) under Program No. P1-0099.

- [1] W. Ho, *J. Chem. Phys.* **117**, 11033 (2002).
- [2] D. M. Eigler and E. K. Schweizer, *Nature (London)* **344**, 524 (1990).
- [3] J. A. Stroscio and D. M. Eigler, *Science* **254**, 1319 (1991).
- [4] M. F. Crommie, C. P. Lutz, and D. M. Eigler, *Phys. Rev. B* **48**, 2851 (1993).
- [5] M. F. Crommie, C. P. Lutz, and D. M. Eigler, *Science* **262**, 218 (1993).
- [6] H. C. Manoharan, C. P. Lutz, and D. M. Eigler, *Nature (London)* **403**, 512 (2000).
- [7] S.-W. Hla, L. Bartels, G. Meyer, and K.-H. Rieder, *Phys. Rev. Lett.* **85**, 2777 (2000).
- [8] J. Lagoute, C. Nacci, and S. Fölsch, *Phys. Rev. Lett.* **98**, 146804 (2007).
- [9] S. Fölsch, P. Hyldgaard, R. Koch, and K. H. Ploog, *Phys. Rev. Lett.* **92**, 056803 (2004).
- [10] J. Li, W.-D. Schneider, R. Berndt, and B. Delley, *Phys. Rev. Lett.* **80**, 2893 (1998).
- [11] V. Madhavan, W. Chen, T. Jamneala, M. Crommie, and N. S. Wingreen, *Science* **280**, 567 (1998).
- [12] C. F. Hirjibehedin, C. P. Lutz, and A. J. Heinrich, *Science* **312**, 1021 (2006).
- [13] Surface Preparation Laboratory, Penningweg 69 F, 1507 DE Zaandam, The Netherlands.
- [14] M. F. Crommie, C. P. Lutz, and D. M. Eigler, *Nature (London)* **363**, 524 (1993).
- [15] See supplementary material at <http://link.aps.org/supplemental/10.1103/PhysRevLett.104.196102> for details.
- [16] Y. Hasegawa and P. Avouris, *Phys. Rev. Lett.* **71**, 1071 (1993).
- [17] N. Knorr, M. A. Schneider, L. Diekhöner, P. Wahl, and K. Kern, *Phys. Rev. Lett.* **88**, 096804 (2002).
- [18] J. A. Stroscio and R. J. Celotta, *Science* **306**, 242 (2004).
- [19] P. Hohenberg and W. Kohn, *Phys. Rev.* **136**, B864 (1964).
- [20] W. Kohn and L. J. Sham, *Phys. Rev.* **140**, A1133 (1965).
- [21] D. Vanderbilt, *Phys. Rev. B* **41**, 7892 (1990).
- [22] J. P. Perdew, K. Burke, and M. Ernzerhof, *Phys. Rev. Lett.* **77**, 3865 (1996).
- [23] P. Giannozzi and S. Baroni *et al.*, *J. Phys. Condens. Matter* **21**, 395502 (2009).